

Surface-Initiated Reversible Addition–Fragmentation Chain Transfer (RAFT) Polymerization from Fine Particles Functionalized with Trithiocarbonates

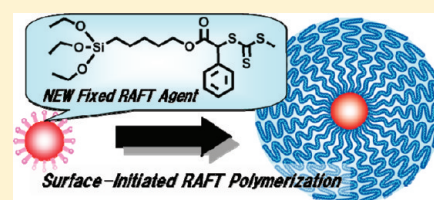
Kohji Ohno,^{*,†} Ying Ma,[†] Yun Huang,[†] Chizuru Mori,[†] Yoshikazu Yahata,[†] Yoshinobu Tsujii,^{†,‡} Thomas Maschmeyer,[§] John Moraes,[§] and Sébastien Perrier[§]

[†]Institute for Chemical Research, Kyoto University, Uji, Kyoto 611-0011, Japan

[‡]JST, CREST, Tokyo 102-0075, Japan

[§]Key Centre for Polymers & Colloids, School of Chemistry, The University of Sydney, Sydney, NSW 2006, Australia

ABSTRACT: Monodisperse silica particles (SiPs) were surface-modified with a newly designed reversible addition–fragmentation chain transfer (RAFT) agent having a triethoxysilane moiety, 6-(triethoxysilyl) 2-(((methylthio)carbonothioyl)thio)-2-phenylacetate (EHT). Surface-initiated RAFT polymerization of styrene was carried out with the EHT-modified SiPs in the presence of a free RAFT agent. The polymerization proceeded in a living manner, producing SiPs coated with well-defined polystyrene of a target molecular weight with a graft density as high as 0.3 chains/nm². Similarly, polymerizations of methyl methacrylate (MMA), *N*-isopropylacrylamide, and *n*-butyl acrylate were conducted, providing SiPs grafted with concentrated (high-density) polymer brushes. In all examined cases, the hybrid particles were highly dispersible in solvents for graft polymers, without causing any aggregations. Owing to exceptionally high uniformity and perfect dispersibility, these hybrid particles formed two- and three-dimensionally ordered arrays at the air–water interface and in suspension, respectively. In addition to the surface-grafting on SiPs, the versatility of this technique was demonstrated by carrying out surface-initiated RAFT polymerization of styrene from iron oxide nanoparticles modified with EHT.



INTRODUCTION

Polymer brushes are macromolecular architectures in which chains of polymer molecules are tethered on one end to a solid surface with a sufficiently high graft density so that the tethered chains are stretched away from the surface. They gather interest from both academia and industry in research fields because of their unique structural features which can provide new insights into polymer science and technology.^{1–12} Among the methodologies of constructing polymer brushes developed so far, surface-initiated living radical polymerization (SI-LRP) is one of the most powerful approaches because of the robustness and versatility inherent to LRP techniques.^{13–17} SI-LRP provides not only excellent control over molecular weight and polydispersity of graft polymers but also a graft density as high as in the “concentrated brush” regime, allowing us to highly functionalize many types of solid surfaces including flat, particle, tubelike, and porous substrates.¹⁸

By using surface-initiated, copper-catalyzed atom transfer radical polymerization (ATRP), we succeeded for the first time in preparing silica particles (SiPs) having a shell layer of a well-defined, high-density (concentrated) poly(methyl methacrylate) (PMMA) brush with no aggregation of particles caused and the narrow distribution of particle size maintained throughout the course of preparation.¹⁷ Thanks to exceptionally high uniformity and good dispersibility, these hybrid particles formed two- and three-dimensionally ordered arrays at the air–water interface and in suspension, respectively.^{19–23} We also applied this technique to nitroxide-mediated LRP system (NMP), preparing monodisperse

fine particles of zinc sulfide core and silica shell grafted with a well-defined polystyrene (PS) brush.²⁴ The PS-grafted hybrid particles also showed perfect dispersibility in solvent for PS and formed well-ordered arrays exhibiting a beautiful structural color. However, ATRP requires the use of a metal catalyst and a ligand, which may contaminate the final product and cause problems for certain applications. NMP permits us to circumvent the use of a catalyst, but it is unfortunately limited in the range of monomers polymerizable by the technique. Therefore, to expand the versatility of the chemistry of surface-grafting polymers, we decided to investigate the possibility of applying reversible addition–fragmentation chain transfer (RAFT) polymerization to surface-initiated polymerization that produces perfectly dispersive and highly uniform hybrid particles grafted with polymer brushes. This is the motivation of the present work.

In addition to the lack of metal catalyst, the major attractions of RAFT polymerization over other LRP techniques include the ability to polymerize a wide range of vinyl monomers, high tolerance to functional groups, and easiness of chain-end functionalization.^{25–28} In fact, RAFT polymerization has been successfully used to prepare polymer brushes using various monomers and various solid substrates.^{18,29} To introduce initiating sites for surface-initiated RAFT polymerization

Received: September 16, 2011

Revised: October 17, 2011

Published: October 31, 2011

on solid substrates, there are mainly two strategies: one is the use of surface-fixed conventional free radical initiators,^{30–32} and the other is the use of surface-fixed RAFT agents.^{33–46} In the latter case, the RAFT agent can be attached to surface via either the Z group^{33–37} or the R group approaches.^{38–46} In the Z group approach, the stabilizing group of RAFT agent is fixed on solid surface so that propagating radicals have to get close to the solid surface across the barrier of polymer brush layer in order to undergo the RAFT reaction during the course of polymerization, typically leading to a lowered graft density. Meanwhile, the R group approach is essentially the same as the so-called grafting-from technique, wherein the RAFT process takes place near the free surface of brush layer. This is a clear advantage over the Z group approach, especially for the synthesis of polymer brushes with a high grafting density. In the present work, therefore, we will focus on the R group approach.

Of the previous instances of surface-initiated RAFT (SI-RAFT) polymerization with the R group approach reported so far, only a few studies used a silane coupling agent bearing RAFT group to directly introduce initiating sites on solid surfaces such as silicon wafer and silica particles.^{38,42} This is probably of several layers of complexity in the chemistry to synthesize a silane coupling agent, including the multistep reaction along with specific experimental conditions for the Grignard reagents. These experimental difficulties have led to the limited spread of SI-RAFT polymerization from a solid substrate modified directly with a silane coupling agent having RAFT moiety. However, this type of silane coupling agent would promisingly further broaden the applicability of SI-RAFT polymerization because of its versatility, that is, the simplicity of surface attachment of RAFT moieties and the availability of various solid substrates to be modified, including silica, alumina, titania, iron oxide, clay, mica, and so on.

In this study, we pursue our first goal of synthesizing a RAFT group-carrying silane coupling agent via a relatively straightforward method. For this purpose, we have chosen a trithiocarbonate group as the basis of the RAFT agent because it can be simply and efficiently incorporated into many organic compounds.²⁸ The second purpose of this work is to fabricate narrowly size-distributed fine particles grafted with a concentrated polymer brush with perfect dispersibility in solvent and also to demonstrate that the polymer brush-afforded hybrid particles form a colloidal crystal because the formation of crystals is believed to be a good measure to verify the quality of the resultant hybrid particles in terms of their dispersibility and uniformity. In what follows, monodisperse SiPs will be surface-modified by a newly designed triethoxysilane derivative having a trithiocarbonate moiety, and the modified SiPs will be used for SI-RAFT polymerizations of various monomers to produce polymer brush-afforded SiPs that have the potential to form colloidal crystals. In addition, iron oxide nanoparticles will also be used as core particles to be grafted with a concentrated polymer brush in order to verify the versatility of the whole processes from the fixation of RAFT agent to the graft polymerization.

EXPERIMENTAL SECTION

Materials. 4-(Dimethylamino)pyridine (DMAP, 99%), α -bromophenylacetic acid (97%), *N,N'*-dicyclohexylcarbodiimide (DCC, 95%), dichloromethane (99%, dehydrated), *N*-isopropylacrylamide (NIPAM, 98%), 2,2'-azobis(isobutyronitrile) (AIBN, 98%), and 1,2-dimethoxyethane (99%) were purchased from Wako Pure Chemicals, Osaka, Japan. 5-Hexen-1-ol (98%) were obtained from Tokyo Chemical Industry, Tokyo, Japan. Sodium

thiomethoxide (95%) was purchased from Aldrich and used without further purification. Carbon disulfide (99%) was obtained from Nacalai Tesque Inc., Osaka, Japan. Styrene (S, 99%), *n*-butyl acrylate (BA, 99%), and methyl methacrylate (MMA, 99%) were obtained from Nacalai Tesque Inc. and purified by flash chromatography over activated neutral alumina. Platinum catalyst (Karstedt's catalyst) solution (Pt-114, platinum content: 3 wt %) was received from Johnson Matthey Catalysts, Royston, UK. Triethoxysilane (99%) was obtained from Chisso Corp., Tokyo, Japan, and distilled before use. Silica particle (SiP) (SEAHOSTER KE-E10, average diameter = 130 nm, 20 wt % suspension of SiP in ethylene glycol) was kindly donated by Nippon Shokubai Co., Ltd., Osaka, Japan. Iron oxide (Fe₃O₄) nanoparticles were prepared by the thermal decomposition of iron oleate complex following the method reported by Hyeon et al.⁴⁷ The average diameter of the Fe₃O₄ nanoparticles was 15 nm as measured by transmission electron microscopy (TEM). Water was purified by a Milli-Q system (Nihon Millipore Ltd., Tokyo, Japan) to a specific resistivity of ca. 18 M Ω ·cm. All other reagents were used as received from commercial sources.

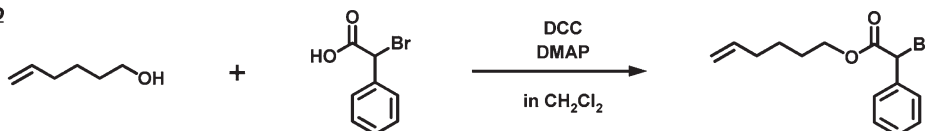
Measurements. Gel permeation chromatographic (GPC) analysis using tetrahydrofuran (THF) as an eluent at a flow rate of 0.8 mL/min was carried out at 40 °C on a Shodex GPC-101 high-speed liquid chromatography system equipped with a guard column (Shodex GPC KF-G), two 30 cm mixed columns (Shodex GPC KF-806 L, exclusion limit = 2×10^7), and a differential refractometer (Shodex RI-101). Polystyrene (PS) standards and poly(methyl methacrylate) (PMMA) standards were used to calibrate the GPC system. This system was used for the characterization of PS, poly(*n*-butyl acrylate) (PBA), and PMMA. GPC analysis using *N,N*-dimethylformamide (DMF) containing 10 mM LiBr as an eluent at a flow rate of 0.8 mL/min was carried out similarly except for the column system, a guard column (Shodex GPC LF-G), and two 30 cm mixed columns (Shodex GPC LF-804, exclusion limit = 2×10^6). This system was calibrated by PMMA standards and used for the characterization of poly(*N*-isopropylacrylamide) (PNIPAM). ¹H (300 MHz) and ¹³C (75 MHz) spectra were obtained on a JEOL/AL300 spectrometer. Elemental analyses were performed at the Laboratory of Elemental Analysis, Institute for Chemical Research, Kyoto University, Japan. The C and H contents were determined by combustion followed by differential thermal conductivity detection using a Microcorder JM10 elemental analyzer (J-Science Lab Co., Ltd., Kyoto, Japan), and the Br contents were determined by combustion followed by ion chromatographic separation and electrical conductivity detection using a XS-100 elemental analyzer (Mitsubishi Chemical Analytech Co., Ltd., Kanagawa, Japan). Dynamic light scattering (DLS) measurements were performed in THF solvent at 20 °C on a DLS-7000 photometer (Otsuka Electronics Co., Ltd., Osaka, Japan) with a He–Ne laser (wavelength 633 nm and power 10 mW) as a light source. The scattering light intensity was measured at a scattering angle of 90°. Data analysis was performed by the histogram method, including non-negative least-squares analysis. Transmission electron microscopic (TEM) observation was made on a JEOL transmission electron microscope JEM-1010 operated at 100 kV. Thermal gravimetric analyses (TGA) were made on a Shimadzu TGA-50 under a nitrogen atmosphere. Confocal laser scanning microscopic (CLSM) observations were made on an inverted-type microscope (LSM 5 PASCAL, Carl Zeiss, Germany) with a 488 nm wavelength Ar laser and $\times 63$ objective (Plan Apochromat, Carl Zeiss) in reflection mode. The distance of the focal plane from the inside surface of the coverslip was 30 μ m.

Preparation of Free RAFT Agent, S-Ethoxycarbonylphenylmethyl Methyltrithiocarbonate (ECPMT, Scheme 1). ECPMT was synthesized via a two-step reaction. First step: α -bromophenylacetic acid (12 g, 55.8 mmol), ethanol (3.9 g, 84.7 mmol), and DMAP (0.68 g, 5.57 mmol) were dissolved in dry dichloromethane (170 mL). The mixture was cooled by ice–water bath, and then DCC (13.9 g, 67.4 mmol) dissolved in dry dichloromethane (50 mL) was added dropwise to the cooled mixture over 30 min. The reaction mixture was magnetically stirred

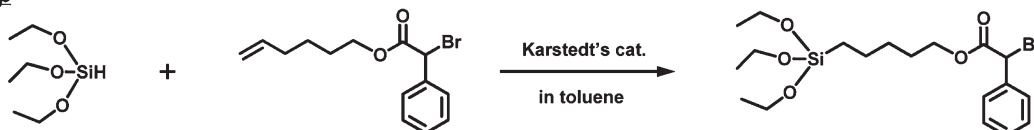
Scheme 1. Synthetic Routes of (a) Fixed RAFT Agent, 6-(Triethoxysilyl)hexyl 2-(((Methylthio)carbonothioyl)thio)-2-phenylacetate (EHT), and (b) Free RAFT Agent, S-Ethoxycarbonylphenylmethyl methyltrithiocarbonate (ECPMT)

(a) Synthesis of EHT

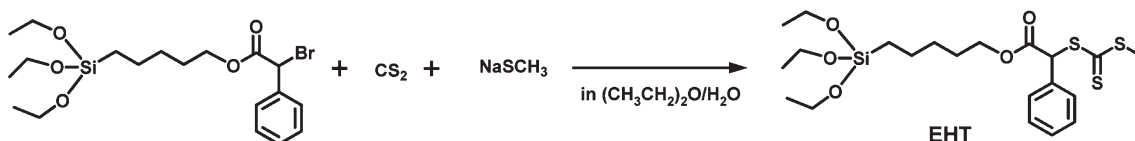
1st step



2nd step

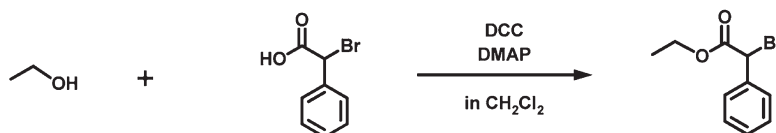


3rd step

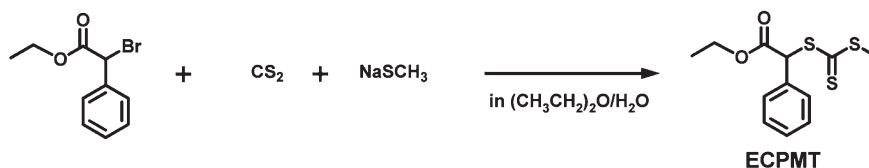


(b) Synthesis of ECPMT

1st step



2nd step



for 24 h at room temperature. The resulting precipitate was removed by filtration, and the filtrate was evaporated to dryness under reduced pressure. The residue was purified by flash chromatography on a column of silica gel with a mixture of *n*-hexane/ethyl acetate = 30/1 as an eluent to yield ethyl α -bromophenylacetate as a transparent liquid (10.9 g, 80% yield). ^1H NMR (CDCl_3): δ 1.27 (t, 3H, CH_3CH_2), 4.26 (q, 2H, CH_3CH_2), 5.3 (s, 1H, CHC_6H_5), 7.30–7.63 (m, 5H, $\text{C}_6\text{H}_5\text{CH}$). ^{13}C NMR (CDCl_3): δ 13.9 (CH_3), 46.9 (CH), 62.5 (CH_2), 128.7, 128.8, 128.9, and 135.9 (C_6H_5), 168.3 ($\text{C}=\text{O}$). Anal. Calcd for $\text{C}_{10}\text{H}_{11}\text{BrO}_2$: C, 49.41; H, 4.56. Found: C, 49.35; H, 4.62.

Second step: carbon disulfide (3.2 g, 42 mmol) in diethyl ether (20 mL) was added to a mixture of sodium thiomethoxide (2.4 g, 34.2 mmol) and water (14 mL) at room temperature. The biphasic solution was vigorously stirred for 4 h, and to which ethyl α -bromophenylacetate (8.5 g, 35 mmol) dissolved in diethyl ether (20 mL) was added dropwise over 30 min. The reaction mixture was stirred at room temperature overnight. The organic layer was collected and washed with saturated brine (3×20 mL). Drying over anhydrous Na_2SO_4 , filtration, and removal of the solvent gave a crude product, which was purified by flash chromatography on a column of silica gel with a mixture of *n*-hexane/ethyl acetate = 15/1 as an eluent to yield ECPMT as a yellow oil (7.02 g, 70% yield). ^1H NMR (CDCl_3): δ 1.27 (t, 3H, CH_3CH_2), 2.72 (s, 3H, CH_3S), 4.20 (m, 2H, CH_3CH_2), 5.80 (s, 1H, $\text{C}_6\text{H}_5\text{CH}$), 7.31–7.47 (m, 5H, $\text{C}_6\text{H}_5\text{CH}$). ^{13}C NMR (CDCl_3): δ 14.0 (CH_3CH_2), 20.2 (CH_3S), 58.2 (CH), 62.5 (CH_2), 128.7, 128.8, 129,

and 133.3 (C_6H_5), 168.8 ($\text{C}=\text{O}$), 222.5 ($\text{C}=\text{S}$). Anal. Calcd for $\text{C}_{12}\text{H}_{14}\text{O}_2\text{S}_3$: C, 50.32; H, 4.93. Found: C, 51.03; H, 5.09.

Synthesis of RAFT Agent Having a Triethoxysilane Moiety, 6-(Triethoxysilyl)hexyl 2-(((Methylthio)carbonothioyl)thio)-2-phenylacetate (EHT, Scheme 1). EHT was synthesized via a three-step reaction. First step: α -bromophenylacetic acid (15.2 g, 70.7 mmol), 5-hexen-1-ol (8.5 g, 84.9 mmol), and DMAP (0.76 g, 6.22 mmol) were dissolved in dry dichloromethane (200 mL). The mixture was cooled by an ice–water bath, and then DCC (16 g, 77.5 mmol) dissolved in dry dichloromethane (60 mL) was added dropwise to the cooled mixture over 30 min. The reaction mixture was magnetically stirred for 24 h at room temperature. The resulting precipitate was removed by filtration, and the filtrate was evaporated to dryness under reduced pressure. The residue was purified by flash chromatography on a column of silica gel with a mixture of *n*-hexane/ethyl acetate = 30/1 as an eluent to yield 5-hexen-1-yl α -bromophenylacetate as a transparent liquid (18.9 g, 90% yield). ^1H NMR (CDCl_3): δ 1.28 (m, 2H, $\text{CH}_2\text{CH}_2\text{CH}=\text{CH}_2$), 1.52 (q, 2H, $\text{CH}_2\text{CH}_2\text{CH}_2\text{CH}=\text{CH}_2$), 2.0 (m, 2H, $\text{CH}_2\text{CH}=\text{CH}_2$), 4.16 (t, 2H, CH_2OOC), 4.96 (m, 2H, $\text{CH}_2=\text{CH}$), 5.27 (s, 1H, CHC_6H_5), 5.60–5.82 (m, 1H, $\text{CH}=\text{CH}_2$), 7.15–7.65 (m, 5H, $\text{C}_6\text{H}_5\text{CH}$). ^{13}C NMR (CDCl_3): δ 24.9 ($\text{CH}_2\text{CH}_2\text{CH}_2\text{CH}=\text{CH}_2$), 27.7 ($\text{CH}_2\text{CH}_2\text{CH}_2\text{CH}=\text{CH}_2$), 30.0 ($\text{CH}_2\text{CH}=\text{CH}_2$), 46.8 (CHC_6H_5), 66.3 (CH_2O), 114.9 ($\text{CH}=\text{CH}_2$), 128.6, 128.7, 129.2, 135.8 (C_6H_5), 138.1 ($\text{CH}=\text{CH}_2$), 168.3 (COO). Anal. Calcd for $\text{C}_{14}\text{H}_{17}\text{BrO}_2$: C, 56.58; H, 5.77; Br, 26.89. Found: C, 56.60; H, 5.77; Br, 26.95.

Second step: 5-hexen-1-yl α -bromophenylacetate (10 g, 33.6 mmol) and dry toluene (130 mL) were charged into a two-neck round-bottom flask equipped with a magnetic stir bar and rubber septum, and the system was deoxygenated by purging with argon. Triethoxysilane (130 mL, 0.7 mol) beforehand purged with argon was added into the flask in a glovebox purged with argon, and subsequently Karstedt's catalyst solution (45 μ L) was added into the system by a syringe. The reaction mixture was magnetically stirred under an argon atmosphere for 24 h. Complete disappearance of 5-hexen-1-yl α -bromophenylacetate, hence the completion of reaction, was confirmed by ^1H NMR spectroscopy. Unreacted triethoxysilane and toluene were completely removed under vacuum by raising the temperature to 60 $^\circ\text{C}$ to yield 6-(triethoxysilyl)hexyl α -bromophenylacetate as a slightly yellow oil in a quantitative yield. ^1H NMR (CDCl_3): δ 0.61 (t, 2H, $\text{CH}_2\text{Si}(\text{OCH}_2\text{CH}_3)_3$), 1.20 (t, 9H, $(\text{CH}_3\text{CH}_2\text{O})_3\text{Si}$), 1.21–1.45 (br, 6H, $\text{CH}_2\text{CH}_2\text{CH}_2\text{CH}_2\text{Si}$), 1.62 (m, 2H, $\text{CH}_2\text{CH}_2\text{O}$), 3.78 (q, 6H, OCH_2CH_3), 4.16 (t, 2H, CH_2O), 5.34 (s, 1H, CHC_6H_5), 7.15–7.65 (m, 5H, $\text{C}_6\text{H}_5\text{CH}$). ^{13}C NMR: 10.2 ($\text{CH}_2\text{Si}(\text{OCH}_2\text{CH}_3)_3$), 18.2 ($(\text{CH}_3\text{CH}_2\text{O})_3\text{Si}$), 22.5 ($\text{CH}_2\text{CH}_2\text{Si}$), 25.2, 28.2, 32.5 (CH_2), 46.8 (CHC_6H_5), 58.1 (OCH_2CH_3), 66.4 (CH_2O), 128.6, 128.7, 129.2, 135.8 (C_6H_5), 168.2 (COO). Anal. Calcd for $\text{C}_{20}\text{H}_{33}\text{BrO}_5\text{Si}$: C, 52.05; H, 7.21; Br, 17.32. Found: C, 52.08; H, 7.11; Br, 17.26.

Third step: carbon disulfide (6.6 g, 86.7 mmol) in diethyl ether (72 mL) was added to a mixture of sodium thiomethoxide (5 g, 71.3 mmol) and water (20 mL) at room temperature. The biphasic reaction mixture was vigorously stirred for 4 h and to which 6-(triethoxysilyl)hexyl α -bromophenylacetate (6 g, 13 mmol) dissolved in diethyl ether (12 mL) was added dropwise over 30 min. The reaction mixture was stirred at room temperature overnight. The organic layer was collected and washed with saturated brine (5 \times 40 mL). Drying over anhydrous Na_2SO_4 , filtration, and removal of the solvent gave 6-(triethoxysilyl)hexyl 2-((methylthio)carbonothioyl)-thio)-2-phenylacetate (EHT) as a yellow liquid in a quantitative yield. ^1H NMR (CDCl_3): δ 0.61 (t, 2H, $\text{CH}_2\text{Si}(\text{OCH}_2\text{CH}_3)_3$), 1.20 (t, 9H, $(\text{CH}_3\text{CH}_2\text{O})_3\text{Si}$), 1.21–1.45 (br, 6H, $\text{CH}_2\text{CH}_2\text{CH}_2\text{CH}_2\text{Si}$), 1.62 (m, 2H, $\text{CH}_2\text{CH}_2\text{O}$), 2.73 (s, 3H, CH_3S), 3.78 (q, 6H, OCH_2CH_3), 4.09–4.20 (m, 2H, CH_2O), 5.81 (s, 1H, CHC_6H_5), 7.32–7.45 (m, 5H, $\text{C}_6\text{H}_5\text{CH}$). ^{13}C NMR: 10.2 ($\text{CH}_2\text{Si}(\text{OCH}_2\text{CH}_3)_3$), 18.2 ($(\text{CH}_3\text{CH}_2\text{O})_3\text{Si}$), 20.1 (CH_3S), 22.5 ($\text{CH}_2\text{CH}_2\text{Si}$), 25.2, 28.2, 32.5 (CH_2), 58.1 (OCH_2CH_3), 58.2 (CHC_6H_5), 66.2 (CH_2O), 128.6, 128.7, 128.8, 133.3 (C_6H_5), 168.8 (OOC), 222.4 ($\text{C}=\text{S}$). Anal. Calcd for $\text{C}_{22}\text{H}_{36}\text{O}_5\text{S}_3\text{Si}$: C, 52.34; H, 7.19; S, 19.06. Found: C, 52.24; H, 7.11; S, 19.20.

Fixation of RAFT Agent on Silica Particles. The suspension of commercially supplied silica particle (SiP) in ethylene glycol was solvent-exchanged to ethanol. Namely, the suspension was diluted with ethanol and centrifuged. The collected SiPs were redispersed in ethanol followed by centrifugation. This cycle was repeated three times to obtain a SiP suspension in ethanol. 1,2-Dimethoxyethane (162 mL), THF (13 mL), and EHT (7 g) were added into the suspension of SiP (4.8 g) in ethanol (24 mL). The suspension in a round-bottomed flask equipped with distillation apparatus was stirred at 90 $^\circ\text{C}$, and the solvent of about 160 mL was removed by azeotropic distillation.^{48,49} The residue was stirred under refluxing at 75 $^\circ\text{C}$ for 12 h. The modified SiPs were washed by consecutive centrifugation and redispersion in ethanol and toluene. Finally, the suspension of the RAFT agent-fixed SiPs was solvent-exchanged to DMF by repeated redispersion/centrifugation to obtain a DMF stock suspension.

Fixation of RAFT Agent on Iron Oxide Nanoparticles. A 100 mL two-necked round-bottom flask equipped with a condenser was charged with a suspension of Fe_3O_4 nanoparticles (200 mg) in THF (16 mL), EHT (400 mg), and triethylamine (400 mg). The mixture was reflux for 24 h, and then additional EHT (200 mg) and triethylamine (400 mg) were added into the reaction system. The mixture was refluxed again for 24 h. The modified Fe_3O_4 nanoparticles were washed by consecutive centrifugation and redispersion in THF to obtain a THF stock suspension.

Surface-Initiated RAFT Polymerization on SiPs. Polymerization of styrene (S) with the RAFT agent EHT-coated SiPs was carried out as follows: the EHT-coated SiPs in DMF were mixed with S containing a prescribed amount of the free RAFT agent of ECPMT. The mother reaction solution was divided nearly equally into a prescribed number of Pyrex glass tubes. The system was degassed by three freeze–pump–thaw cycles and then sealed off under vacuum. The polymerization was carried out in a shaking oil bath (TAITEC Corp., Saitama, Japan, Personal H-10) thermostated at 110 $^\circ\text{C}$ and, after a predetermined time t , quenched to room temperature. An aliquot of the solution was taken out for NMR measurement to estimate monomer conversion. The rest of the reaction mixture was diluted by THF and centrifuged to collect polymer-grafted SiPs. The supernatant was used for GPC measurements to determine molecular weight and its distribution of the free polymers. The cycle of centrifugation and redispersion in THF was repeated five times to obtain polymer-grafted SiPs perfectly free of the unbound (free) polymer. To determine the molecular weight of the graft polymer, PS chains were cleaved from the surface as follows: the polymer-grafted SiPs (25 mg) and tetraoctylammonium bromide (50 mg), as a phase transfer catalyst, were dissolved in toluene (5 mL), to which a 10% HF aqueous solution (5 mL) was added. The mixture was vigorously stirred for 3 h. The cleaved polymer in the organic layer was subjected to GPC measurements. To estimate the amount of graft polymer, hybrid particles were subjected to thermal gravimetric analysis. In a typical run, the polymerization of S was carried out at 110 $^\circ\text{C}$ for 11 h with the starting materials S (1.78 g, 17 mmol), ECPMT (1.2 mg, 4.2 μmol), EHT-fixed SiPs (20 mg), and DMF (200 mg). This gave a monomer conversion of 44%, a free polymer with $M_n = 109\,000$ and $M_w/M_n = 1.42$, and a graft polymer with $M_n = 166\,000$ and $M_w/M_n = 1.20$, where M_n and M_w are the number- and weight-average molecular weights, respectively, and M_w/M_n is the polydispersity index.

For BA polymerization, the EHT-coated SiPs in DMF were mixed with BA containing a prescribed amount of ECPMT and AIBN. The mother reaction solution was divided nearly equally into a prescribed number of Pyrex glass tubes. The system was degassed by three freeze–pump–thaw cycles and then sealed off under vacuum. The polymerization was carried out at 60 $^\circ\text{C}$ in a similar procedure as the S polymerization described above. The graft polymer was cleaved from the surface in the similar way to the cleaving of PS grafts as described above. In a typical run, the polymerization of BA was carried out at 60 $^\circ\text{C}$ for 6 h with the starting materials BA (6.25 g, 49 mmol), ECPMT (14 mg, 49 μmol), AIBN (1.6 mg, 9.7 μmol), EHT-fixed SiPs (125 mg), dioxane (6.25 mL), and DMF (750 mg). This gave a monomer conversion of 69%, a free polymer with $M_n = 86\,400$ and $M_w/M_n = 1.27$, and a graft polymer with $M_n = 94\,700$ and $M_w/M_n = 1.08$.

For MMA polymerization, the EHT-coated SiP in DMF was solvent-exchanged to MMA to obtain a 1 wt % suspension in MMA. The suspension was mixed with a prescribed amount of the free RAFT agent ECPMT and AIBN. The polymerization was carried out at 60 $^\circ\text{C}$ in a similar way to the polymerization of S described above. The graft polymer was cleaved in a similar way to the cleaving of PS grafts as described above. In a typical run, the bulk polymerization of MMA was carried out at 60 $^\circ\text{C}$ for 6 h with the starting materials MMA (2 g, 19.98 mmol), ECPMT (2.8 mg, 10 μmol), AIBN (0.32 mg, 2 μmol), and EHT-fixed SiPs (20 mg). This gave a monomer conversion of 18%, a free polymer with $M_n = 90\,800$ and $M_w/M_n = 1.60$, and a graft polymer with $M_n = 48\,700$ and $M_w/M_n = 1.47$.

For NIPAM polymerization, the EHT-coated SiP in DMF was solvent-exchanged to dioxane. The suspension was mixed with a prescribed amount of NIPAM, ECPMT, and AIBN. The solution polymerization of NIPAM (30 wt %) in dioxane was carried out at 60 $^\circ\text{C}$ in the similar procedure as the polymerizations described above. The PNIPAM chains were cleaved from the surface as follows: the PNIPAM-grafted SiPs (25 mg) were dispersed in acetone (5 mL), to

which a 10% HF aqueous solution (5 mL) was added. The mixture was vigorously stirred for 1.5 h. The system was neutralized by NaHCO_3 and diluted with DMF. The cleaved polymer in the solution was subjected to GPC measurements. In a typical run, the solution polymerization of NIPAM was conducted at 60 °C for 5 h with the starting materials NIPAM (1 g, 8.84 mmol), ECPMT (1.27 mg, 4.42 μmol), AIBN (0.15 mg, 0.88 μmol), EHT-fixed SiPs (20 mg), and dioxane (2.3 g). This gave a monomer conversion of 59%, a free polymer with $M_n = 106\,000$ and $M_w/M_n = 1.33$ and a graft polymer with $M_n = 113\,000$ and $M_w/M_n = 1.33$.

RESULTS AND DISCUSSION

Synthesis of Silane Coupling Agent Having RAFT Moiety.

In previous studies, we synthesized triethoxysilane derivatives having an initiating site for atom transfer radical or nitroxide-mediated polymerizations.^{17,24} The reaction with the triethoxysilane group can be carried out in polar solvents such as ethanol and methanol. This is a clear advantage for achieving a homogeneous modification of SiP surface because SiP exhibits higher dispersibility in polar solvents than in apolar ones due to the hydrophilic character of SiP surfaces with silanol groups. In addition, we have chosen a trithiocarbonate group as a RAFT group because of the simplicity for the synthesis of its derivatives.²⁸ Therefore, we have here decided to synthesize a triethoxysilane derivative having a trithiocarbonate group.

The desired compound was synthesized via the three-step reaction described in the Experimental Section (see Scheme 1): in short, 5-hexen-1-ol was acylated with α -bromophenylacetic acid using DCC to obtain 5-hexen-1-yl α -bromophenylacetate, the aryl group of which was subsequently hydrosilylated with triethoxysilane in the presence of Karstedt's catalyst to obtain 6-(triethoxysilyl)hexyl α -bromophenylacetate. Finally, it was reacted with sodium methyl trithiocarbonate prepared from carbon disulfide and sodium thiomethoxide to yield 6-(triethoxysilyl)hexyl 2-(((methylthio)carbonothioyl)thio)-2-phenylacetate (EHT). There are some reasons for the reaction to be carried out in this order: first, the activity of Karstedt's catalyst is significantly lowered by calcogen-containing compounds such as the trithiocarbonate derivative used here.^{50,51} Second, the triethoxysilane group is relatively stable even in the presence of a limited amount of water. In fact, no hydrolysis of the triethoxysilane group was observed in the final step in which a biphasic (water/diethyl ether) system was used as a reaction medium. The overall yield was relatively high, and the purity of the final product EHT was confirmed to be more than 95% by ^1H and ^{13}C NMR and elemental analysis. We selected a phenylacetate as a leaving group as it had been shown to provide excellent control of polymerization over a range of monomers;⁵² a secondary carbon on the active center reduces steric hindrance of the propagating species, thus allowing for fast addition to monomer, while the presence of a phenyl group increases the stability of the generated radical, thus enhancing fragmentation.

Fixation of RAFT Agent on SiP. In our previous work, silane coupling agents having an initiating site for ATRP or NMP were fixed onto SiP surface in ethanol solution with NH_3 added as an alkaline catalyst.^{17,24} The RAFT agent EHT, however, cannot be fixed in a similar way because NH_3 decomposes trithiocarbonate moiety producing a thiol via aminolysis. Yoshinaga et al. previously reported that, in the modification of SiP with some alkoxy silane compounds, azeotropic removal of alcohol and water produced during the reaction gave an effective attachment of the silane coupling agents to the surface of SiP.^{48,49} Following

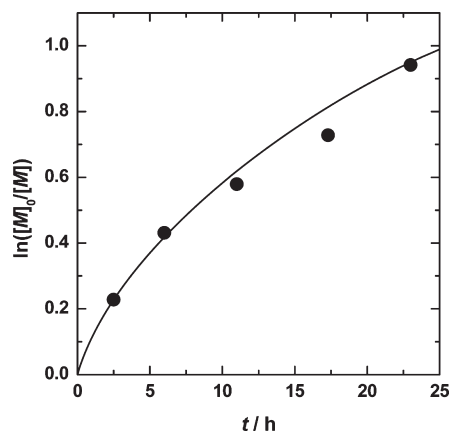


Figure 1. Plot of $\ln([M]_0/[M])$ vs polymerization time t for the solution polymerization of styrene (S) in N,N -dimethylformamide (10 wt %) at 110 °C with RAFT agent-fixed silica nanoparticles (1 wt %): $[S]_0/[free\ RAFT\ agent\ ECPMT]_0 = 4000/1$.

this method, we carried out the surface modification of SiP with EHT (see Experimental Section). To estimate the amount of RAFT agent fixed on SiP, we carried out an elemental analysis of the modified SiPs and determined the sulfur content to be 0.3%, which, along with the known density (1.9 g/cm^3) and the diameter (130 nm) of the SiP, led to a surface density of 0.8 trithiocarbonate group/ nm^2 . After the fixation of RAFT agent, the SiPs became pale yellow and showed good dispersibility in many organic solvents such as acetone, THF, DMF, and so on. The suspension of the modified SiPs could be stably stored in a refrigerator without any change for at least 6 months.

Surface-Initiated RAFT Polymerization of Styrene from SiPs. The EHT-fixed SiP was subsequently used for the RAFT polymerization of styrene (S). To obtain a satisfactory result, we carried out the polymerization in the presence of a free RAFT agent, ECPMT. The role of the free RAFT agent is to allow an efficient exchange reaction between graft and free polymers so as to control the polymerization, i.e., to yield low-polydispersity polymers. Another role of the free RAFT agent is to prevent interparticle coupling, causing gelation or particle aggregation because free polymers produced by the free RAFT agent will increase the viscosity of the polymerization system, through which the particles have difficulty diffusing. In addition, we added DMF (10 wt %) to the polymerization system in order to obtain good dispersibility of the EHT-fixed SiPs. It is worth mentioning that when the bulk polymerization of S was carried out in the presence of the EHT-fixed SiPs, a small part of the particles formed aggregates.

Figure 1 shows the first-order kinetic plot of monomer concentration for the solution polymerization of S in DMF with the free RAFT agent ECPMT in the presence of the EHT-functionalized SiPs. The plot is not linear and curves slightly downward as the polymerization proceeds. This indicates that the number of propagating radical species in the system does not remain constant throughout the course of polymerization. This can be explained by the decreasing rate of thermal initiation of S with increasing conversion and decreasing monomer concentration. The SiPs purified after the polymerization were treated with HF to cleave the graft polymer from the surface for subsequent GPC analysis.

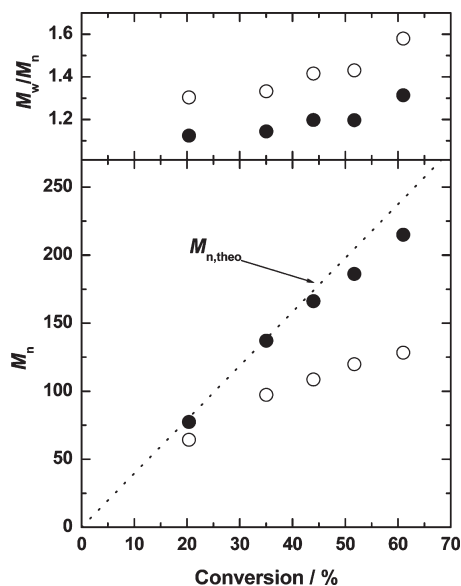


Figure 2. Evolution of number-average molecular weight (M_n) and polydispersity index (M_w/M_n) of the graft (●) and free (○) polymers as a function of monomer conversion for solution polymerization of styrene (S) in *N,N*-dimethylformamide (10 wt %) at 110 °C with RAFT agent-fixed silica nanoparticles (1 wt %): $[S]_0/[free\ RAFT\ agent\ ECPMT]_0 = 4000/1$.

Figure 2 presents the evolution of the number-average molecular weight M_n and the polydispersity index M_w/M_n of the cleaved graft polymer and of the free polymer simultaneously produced from the free RAFT agent ECPMT as a function of monomer conversion. The dotted line shows the theoretical value of M_n ($M_{n,theo} = M_S \times C \times \{[S]_0/([ECPMT]_0 + [trithiocarbonate\ groups\ on\ SiP\ available\ for\ the\ surface\ grafting]_0)\}$), where M_S is the molecular weight of S, C is the conversion, and $[S]_0$ and $[ECPMT]_0$ are the concentration of S and ECPMT in feed, respectively. The fraction of trithiocarbonate groups on SiP used for the surface grafting was estimated by polymer grafting density, as will be described below. The M_n values progressively deviate from the $M_{n,theo}$, and this was more evident for the free polymer than for the graft polymer. This is probably because the thermal initiation of S creates additional free chains. As already mentioned, this thermal initiation is also responsible for the nonlinearity of the first-order kinetic plot of monomer concentration. Indeed, the maximum amount of polymer radicals thermally produced is 1.5×10^{-3} mol/L,^{53,54} which amounts to about 60% of the initial concentration of trithiocarbonate groups in this case ($[ECPMT]_0 + [trithiocarbonate\ groups\ on\ SiP\ available\ for\ the\ surface\ grafting]_0 = 2.4 \times 10^{-3}$ mol/L). The M_w/M_n ratio remains low up to 50% conversion, around 1.2 for the graft polymers and 1.4 for the free polymers. The relatively large polydispersity index of the free polymer can also be explained by the contribution of the thermal initiation of S creating additional free polymer chains. Nonetheless, all these results confirm that the RAFT polymerization of S initiated from the surface of SiPs proceeds in a living fashion, giving SiPs with well-defined SiP (PS-SiPs).

Polymer Grafting Density. Thermogravimetric analysis for the PS-SiPs prepared above was carried out to estimate the mass (w) of polymer grafted on the SiPs. The graft density (σ) was

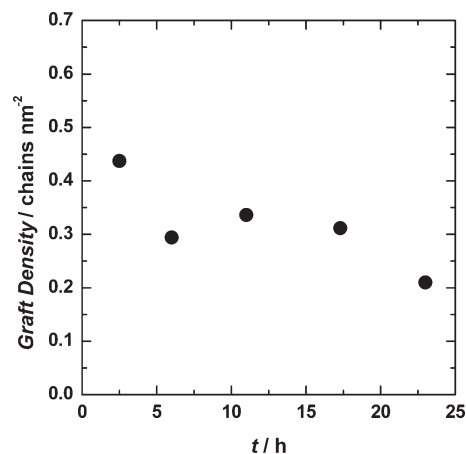


Figure 3. Time dependence of the graft density of polystyrene grown from the surfaces of silica particles.

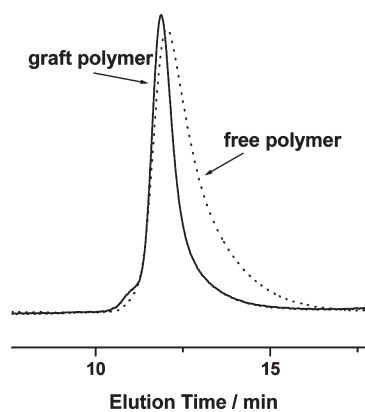


Figure 4. Gel permeation chromatographic traces for the graft (solid curve) and free (broken curve) polymers at 17 h of polymerization of styrene (S) in *N,N*-dimethylformamide (10 wt %) at 110 °C with RAFT agent-fixed silica nanoparticles (1 wt %): $[S]_0/[free\ RAFT\ agent\ ECPMT]_0 = 4000/1$.

then calculated by eq 1

$$\sigma = (w/M_n)A_v/(\pi d_c^2) \quad (1)$$

where A_v is Avogadro's number and d_c is the diameter of the SiP core. In the estimation, the density of the SiP was set to be 1.9 g/cm³. Figure 3 shows that the graft density ranges from 0.2 to 0.5 chains/nm², which means that PS chains have grown from about half of the trithiocarbonate groups fixed on the SiP surface. It can also be seen that the graft density tends to decrease gradually with increasing the polymerization time. We previously reported that in surface-initiated RAFT polymerization mediated via dithiobenzoate as a chain transfer group the graft density of PS chains decreased with the polymerization time rather sharply at first and then slowly.⁴¹ This was interpreted as a result of the enhanced recombination of polymer radicals being due to the migration of radicals on the surface by sequential chain transfer reactions. In fact, in the graft polymerization, a shoulder peak, assignable to dead chains produced by recombination of polymer radicals, was conspicuously observed in the GPC traces of the graft polymers. However, in the present system, almost no such shoulder is detectable in the GPC traces of both the graft and free polymers,

as shown in Figure 4. This means that the phenomenon of decreasing graft density shown in Figure 3 does not come from the enhanced recombination of polymer radicals on the surface, but the reason for this is not at present clear. Importantly, the graft densities obtained here are high enough to demonstrate that the layer of polymer grafts is in the concentrated-brush regime.

DLS Measurements of PS-SiPs. The PS-SiPs obtained here are easily dispersed in most common solvents for PS. DLS measurements were conducted for a series of hybrid particles in a dilute THF solution. Figure 5 shows the hydrodynamic diameters D_h for the hybrid PS-SiPs as a function of M_n of the PS grafts. The diameters of the compact-core shell model⁵⁵ and the fully stretched core-shell model⁵⁵ are also shown in the figure. The former model consists of a SiP core and a PS shell of bulk density, and the latter one consists of a SiP core and a PS shell whose size is equal to that of the PS chains radially stretched in all-trans conformation. The D_h value increases with increasing M_n , being intermediate between the diameters of the two models. Importantly, the relative standard deviation δ remained nearly constant around 5% for most samples as shown in Figure 5. The D_h and δ of the EHT-functionalized SiPs were 145 nm and 5.2%, respectively, indicating that the particles retained high dispersibility throughout the experimental processes from the initiator fixation to graft polymerization.

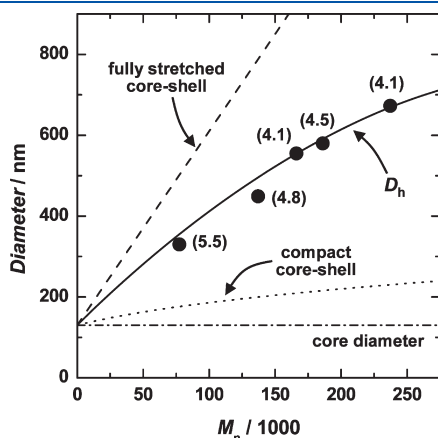


Figure 5. Plot of average hydrodynamic diameter D_h of silica particles grafted with polystyrene (PS-SiP) as a function of number-average molecular weight M_n of the PS graft chains. The D_h values were determined by dynamic light scattering in dilute THF suspension at 20 °C. The diameters of SiP cores are 130 nm. The broken and dotted lines represent the diameters of the fully stretched and compact core-shell models, respectively (see text).⁵⁵ The numbers in parentheses represent the relative standard deviation of particle size.

Two-Dimensional Ordered Arrays of PS-SiPs. The monolayers of PS-SiPs were prepared following a previously reported procedure.^{17,19} Briefly, a droplet of a concentrated suspension of PS-SiPs in toluene was deposited onto the surface of purified water, giving a thin film at the air–water interface as the toluene evaporated. This thin film was transferred onto a TEM grid. Figure 6 shows TEM images of the transferred monolayers for PS-SiPs with a core diameter of 130 nm and different molecular weights of PS grafts ($M_n =$ (a) 31 000 and (b) 137 000). In both cases, the SiPs cores, visible as dark circles, are uniformly dispersed without causing any aggregation, while the PS chains, which should form fringes surrounding the SiP cores, are hardly seen because of their low electron density. The center-to-center distance between the nearest-neighbor particles increased with increasing molecular weight of graft chains.

Formation of Colloidal Crystals. We previously identified a colloidal crystal in a suspension of hybrid particles having a spherical silica core and a shell of well-defined PMMA concentrated brush.^{20–22} Following a similar procedure, fabrication of a colloidal crystal was attempted using the PS-SiPs prepared in the present work. Briefly, the PS-SiP hybrid particles used here have a SiP core of average diameter 130 nm and a shell of PS graft chains of $M_n = 130\,000$ and $M_w/M_n = 1.15$, end-grafted on the SiP surface with a surface density as high as 0.3 chains/nm². The hybrid particles were suspended in a mixture of chlorobenzene/*o*-dichlorobenzene of volume composition 70/30. The particle suspension of 12.9 vol % was allowed to stand at ambient temperature. Tiny iridescent flecks were observed several tens of minutes after the onset of the experiment, indicating the formation of Bragg-reflecting crystallites, and the formed crystallites filled the whole volume of the suspension, as shown in Figure 7.

The PS-SiNP suspension was subjected to confocal laser scanning microscopic (CLSM) measurement to examine the crystal structure visually. Figure 8 shows a CLSM image of a two-dimensional slice inside the sample. The SiP cores of the hybrid particles are clearly visible as yellow dots forming a two-dimensional square lattice, while the PS brush layers are hardly visible because of their much lower reflectivity. Assuming that the CLSM image represents the (100) crystalline plane of face-centered cubic (fcc) structure, according to our previous study,²² the mean nearest-neighbor center-to-center distance D_{dis} between particles was found to be 380 nm (Figure 8). The distance can also be estimated from the particle volume fraction ϕ in the crystal, according to the following relation, which is valid for closed-packed structures:^{21,22}

$$D_{dis, cal} = 2^{1/6}(V_p/\phi)^{1/3} \quad (2)$$

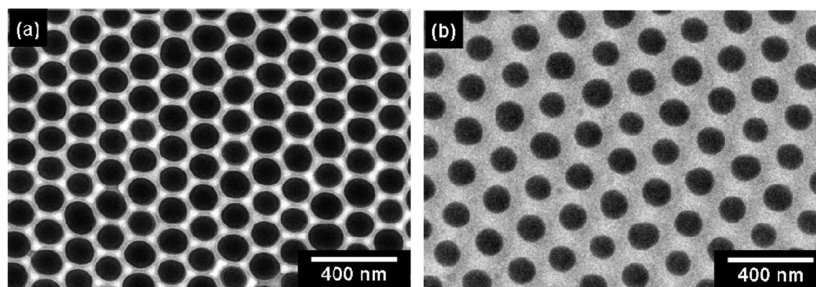


Figure 6. Transmission electron microscopic images of the transferred films of silica particles end-grafted with polystyrene brushes (PS-SiPs): the average diameter of the silica particle cores is 130 nm. Number-average molecular weights of the graft polymers are (a) 31 000 and (b) 137 000.

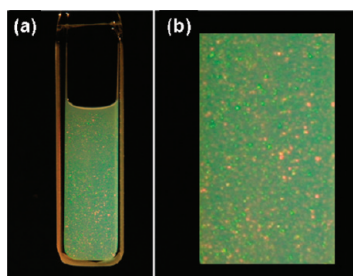


Figure 7. Photographs of a suspension of silica particles end-grafted with polystyrene brush (PS-SiP) in a mixed solvent (chlorobenzene/1,2-dichloroethane, 70/30 volume ratio) illuminated from behind by white light. The number-average molecular weight of the PS grafts is 130 000, and the average diameter of the SiP core is 130 nm. The weight fraction of PS-SiP was 12.9 vol %. (b) is a close-up of (a).

where V_p is the volume of a PS-SiP particle in units of nm^3 . The $D_{\text{dis,cal}}$ value was calculated to be 370 nm, which is in good agreement with the experimentally observed D_{dis} value. This suggests the validity of our assumption for the crystalline structure. The D_{dis} value has a good correlation with the hydrodynamic diameter $D_h = 400$ nm of the hybrid particle determined in dilute suspension. This confirms the uniformity of the crystal as well as the consistency of the relevant experimental procedures. The crystal formation strongly supports the high uniformity and perfect dispersibility of the hybrid particles prepared by the surface-initiated RAFT polymerization from SiPs functionalized with a newly designed RAFT agent with a triethoxysilane.

Application to Various Monomers. The results of S polymerization have encouraged us to extend this grafting technique to various monomers. Table 1 summarizes the results on polymerizations of *n*-butyl acrylate (BA), *N*-isopropylacrylamide (NIPAM), and methyl methacrylate (MMA). The solution polymerization of BA was carried out with 1 wt % of the EHT-functionalized SiP and the initial molar ratio of $[\text{BA}]_0:[\text{ECPMT}]_0:[\text{AIBN}]_0 = 1000:1:0.2$ in dioxane (50 wt %) at 60 °C (see runs 1–4 in Table 1). The polymerization shows a good control and leads to free and graft polymers with molecular weights close to the expected ones and relatively low M_w/M_n around 1.2. The graft density is approximately equal to 0.3 chains/ nm^2 , which is nearly the same as the value about 0.3 chains/ nm^2 for the S polymerization described above.

NIPAM polymerization was carried out with 1 wt % of the EHT-functionalized SiP and the initial molar ratio of $[\text{NIPAM}]_0:[\text{ECPMT}]_0:[\text{AIBN}]_0 = 2000:1:0.2$ in dioxane (70 wt %) at 60 °C (see runs 5–7 in Table 1). In this polymerization, the induction period where the monomer conversion hardly increases was observed during the first few hours of the polymerization time,⁵⁶ after which the polymerization proceeded in a well-controlled fashion. The graft density of PNIPAM brushes is about 0.3 chains/ nm^2 , which is nearly the same as those for PS and PBA brushes described above.

MMA polymerization was carried out with 1 wt % of the EHT-functionalized SiP and the initial molar ratio of $[\text{MMA}]_0:[\text{ECPMT}]_0:[\text{AIBN}]_0 = 2000:1:0.2$ in bulk at 60 °C (see runs 8–10 in Table 1). The polymerization is much slower than for the other monomers and shows a poor control, resulting in polymers with molecular weights deviating from the theoretical value and with broad molecular weight distribution (M_w/M_n) around 1.5 for most samples. Poor control over MMA polymerization was also observed in the RAFT polymerization of MMA

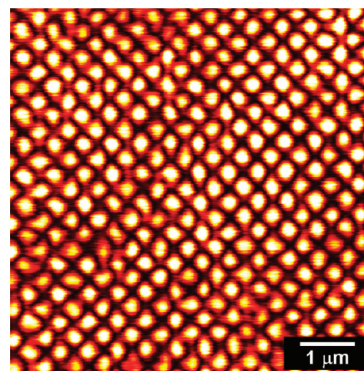


Figure 8. Confocal laser scanning microscopic image of colloidal crystal of silica nanoparticles end-grafted with polystyrene brush (PS-SiPs). Observation was performed using an Ar laser of wavelength 488 nm and $\times 63$ objective in reflection mode. The distance of the focal plane from the inside of the coverslip was 30 μm . The diameter of the SiP cores is 130 nm. The number-average molecular weight of the PS graft is 130 000. The mean nearest-neighbor interparticle distance is 380 nm.

with *S*-methoxycarbonylphenylmethyl methyltrithiocarbonate,⁵² which is similar in structure to the RAFT agent used in this work. Indeed, trithiocarbonates are known to provide poor control over MMA polymerization. In addition, surprisingly, molecular weights of the graft polymers clearly differ from those of the free polymers. The reason is still not clear at present. Nonetheless, PMMA brushes can be obtained with a moderately high graft density around 0.3 chains/ nm^2 .

Application to Iron Oxide Nanoparticles. Silane coupling agents can generally be used for the surface modification not only of silica but also of other metal oxides such as titanium oxide, aluminum oxide, and iron oxide. In this study, to demonstrate the versatility of the silane coupling agent of EHT, we have tried to modify a surface of iron oxide (Fe_3O_4) nanoparticle with the fixed RAFT agent and to achieve SI-RAFT polymerization using the thus-modified Fe_3O_4 nanoparticles. The nanoparticles were prepared following the method previously reported by Hyeon et al. in which thermal decomposition of iron–oleate complex was conducted in high boiling solvent to obtain monodisperse Fe_3O_4 nanoparticles with varying sizes depending on solvents and temperatures used for the synthesis. We carried out the reaction in trioctylamine as a solvent so as to obtain Fe_3O_4 nanoparticles with average diameter of 15 nm. The dispersibility of the Fe_3O_4 nanoparticles in the mixed solvent used for the surface modification of SiPs with EHT was not high enough to obtain a perfectly homogeneous dispersion. This is probably because that the Fe_3O_4 nanoparticle is stabilized with oleic acid, so that the reaction with EHT was instead performed in THF. In order to introduce a sufficiently large amount of RAFT groups on the surfaces of Fe_3O_4 nanoparticles, two further modifications to the procedure used for SiP surfaces were needed: triethylamine was added as a basic catalyst to the reaction system, and also additional triethylamine and EHT were added 24 h after the start of reaction. Without these steps, subsequent graft polymerization did not give a satisfactory result, namely, the graft density obtained was rather low of around 0.01 chains/ nm^2 .

The Fe_3O_4 nanoparticles modified as described above were then subjected to SI-RAFT polymerization of BA in DMF (20 wt %) at 60 °C for 15 h with the initial molar ratio of $[\text{BA}]_0:[\text{ECPMT}]_0:[\text{AIBN}]_0 = 1000:1:0.2$. The polymerization proceeded in a living fashion, producing Fe_3O_4 nanoparticles grafted

Table 1. Results on Surface-Initiated RAFT Polymerizations of *n*-Butyl Acrylate (BA), *N*-Isopropylacrylamide (NIPAM), and Methyl Methacrylate (MMA) on Silica Particles

run	monomer	polymerization time (h)	monomer conversion (%)	$M_{n,theo}$	free polymer		graft polymer		graft density (chains/nm ²)
					M_n	M_w/M_n	M_n	M_w/M_n	
1 ^a	BA	2	21	26 900	39 100	1.19	27 700	1.09	0.31
2 ^a	BA	4	55	70 600	78 100	1.20	73 600	1.30	0.36
3 ^a	BA	6	69	88 000	86 400	1.27	94 700	1.08	0.31
4 ^a	BA	7.5	76	97 600	105 000	1.24	100 000	1.07	0.31
5 ^b	NIPAM	4.5	51	116 000	99 000	1.26	87 000	1.22	0.32
6 ^b	NIPAM	5	59	134 000	106 000	1.33	113 000	1.33	0.31
7 ^b	NIPAM	6	75	170 000	119 000	1.41	106 000	1.23	0.27
8 ^c	MMA	2	6	12 700	83 000	1.63	17 600	1.37	0.38
9 ^c	MMA	4	15	30 000	84 900	1.65	34 400	1.54	0.33
10 ^c	MMA	6	18	36 000	90 800	1.60	48 700	1.47	0.36

^a Polymerizations were carried out in dioxane (50 wt %) at 60 °C with RAFT agent-fixed silica nanoparticles (1 wt %): [*n*-butyl acrylate]₀/[free RAFT agent ECPMT]₀/[AIBN]₀ = 1000/1/0.2. ^b Polymerizations were carried out in dioxane (70 wt %) at 60 °C with RAFT agent-fixed silica nanoparticles (1 wt %): [*N*-isopropylacrylamide]₀/[free RAFT agent ECPMT]₀/[AIBN]₀ = 2000/1/0.2. ^c Polymerizations were carried out in bulk at 60 °C with RAFT agent-fixed silica nanoparticles (1 wt %): [methyl methacrylate]₀/[free RAFT agent ECPMT]₀/[AIBN]₀ = 2000/1/0.2.

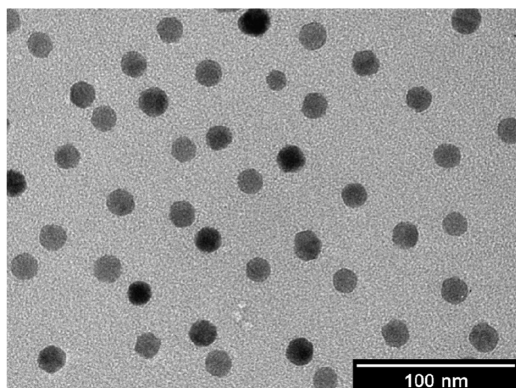


Figure 9. Transmission electron microscopic image of the transferred films of iron oxide nanoparticles end-grafted with poly(*n*-butyl acrylate) brushes: the average diameter of the iron oxide nanoparticle cores is 15 nm. Number-average molecular weight of the graft polymers is 139 000.

with low-polydispersity polymers with $M_n = 139\,000$ and $M_w/M_n = 1.18$. The graft density was estimated to be about 0.1 chains/nm², which is somewhat lower than that of the PBA grafting on the SiPs. This may come from some experimental error in determining the diameter of the Fe₃O₄ nanoparticles and also from a low covering of RAFT residues on the nanoparticles. Nonetheless, the graft density is high enough to support the production of concentrated polymer brush. These hybrid particles had an exceptionally high dispersibility in organic solvents for PBA. Figure 9 shows a typical TEM image of a cast film of the Fe₃O₄ nanoparticles grafted with the PBA chains. It can be seen that each particle individually dispersed in the film without causing any aggregates. This system with Fe₃O₄ nanoparticles will be readily applicable to polymerizations of a broad range of monomers as demonstrated in the system with SiPs described above. Furthermore, by combining with the magnetic property of Fe₃O₄ nanoparticles, the hybrids will be useful for many applications,⁵⁷ for instance, magnetic separation and magnetic resonance imaging.

CONCLUSIONS

Monodisperse SiPs with a diameter of 130 nm were surface-modified with a newly designed triethoxysilane having trithiocarbonate group for RAFT polymerization. The modification was carried out by azeotropic removal of ethanol and water produced during the reaction, without the use of ammonia, a well-known catalyst for the reaction with alkoxy silanes, which decomposes the trithiocarbonate group. The surface-initiated RAFT polymerization of S was achieved with good control over the molecular weight and molecular weight distribution of the graft polymer and with a high graft density around 0.3 chains/nm². This grafting technique mediated by RAFT polymerization was successfully applied to other monomers and also iron oxide nanoparticles as a solid substrate. The resultant hybrid particles had high uniformity and high dispersibility. Combining these features and the advantages of RAFT polymerization such as tolerance to functional groups and rich chemistry in chain-end functionalization, the present system will provide intriguing polymer-brush surfaces leading to unique applications.

AUTHOR INFORMATION

Corresponding Author

*E-mail: ohno@scl.kyoto-u.ac.jp.

ACKNOWLEDGMENT

This work was supported in part by a Grant-in-Aid for Scientific Research (Grant-in-Aid 17685010 and 23685049) from the Ministry of Education, Culture, Sports, Science, and Technology, Japan, and by Industrial Technology Research Grant Program in 2004 and 2009 from the New Energy and Industrial Technology Development Organization (NEDO) of Japan. J.M. gratefully acknowledges funding from the O'Donnell Young Scientist Prize.

REFERENCES

- (1) Advincula, R. C.; Brittain, W. J.; Baster, K. C.; Ruhe, J. *Polymer Brushes: Synthesis, Characterization, Applications*; Wiley-VCH Verlag GmbH & Co. KGaA: Weinheim, 2004; p 483.

- (2) Jordan, R. Ed.; Surface-Initiated Polymerization II. *Adv. Polym. Sci.* **2006**, *198*, 214.
- (3) Jordan, R. Ed.; Surface-Initiated Polymerization I. *Adv. Polym. Sci.* **2006**, *197*, 202.
- (4) Bhattacharya, A.; Misra, B. N. *Prog. Polym. Sci.* **2004**, *29*, 767–814.
- (5) Gupta, B.; Anjum, N. *Adv. Polym. Sci.* **2003**, *162*, 35–61.
- (6) Ito, Y.; Park, Y. S. *Polym. Adv. Technol.* **2000**, *11*, 136–144.
- (7) Kim, J.-H.; Park, K.; Nam, H. Y.; Lee, S.; Kim, K.; Kwon, I. C. *Prog. Polym. Sci.* **2007**, *32*, 1031–1053.
- (8) Nasef, M. M.; Hegazy, E.-S. A. *Prog. Polym. Sci.* **2004**, *29*, 499–561.
- (9) Padeste, C.; Farquet, P.; Potzner, C.; Solak, H. H. *J. Biomater. Sci., Polym. Ed.* **2006**, *17*, 1285–1300.
- (10) Ruhe, J.; Ballauff, M.; Biesalski, M.; Dziezok, P.; Groehn, F.; Johannsmann, D.; Houbenov, N.; Hugenberg, N.; Konradi, R.; Minko, S.; Motornov, M.; Netz, R. R.; Schmidt, M.; Seidel, C.; Stamm, M.; Stephan, T.; Usov, D.; Zhang, H. *Adv. Polym. Sci.* **2004**, *165*, 79–150.
- (11) Ruhe, J.; Knoll, W. *J. Macromol. Sci., Polym. Rev.* **2002**, *C42*, 91–138.
- (12) Uyama, Y.; Kato, K.; Ikada, Y. *Adv. Polym. Sci.* **1998**, *137*, 1–39.
- (13) Zhou, F.; Huck, W. T. S. *Phys. Chem. Chem. Phys.* **2006**, *8*, 3815–3823.
- (14) Edmondson, S.; Osborne, V. L.; Huck, W. T. S. *Chem. Soc. Rev.* **2004**, *33*, 14–22.
- (15) Tsujii, Y.; Ohno, K.; Yamamoto, S.; Goto, A.; Fukuda, T. *Adv. Polym. Sci.* **2006**, *197*, 1–45.
- (16) Fukuda, T.; Tsujii, Y.; Ohno, K. *Macromol. Eng.* **2007**, *2*, 1137–1178.
- (17) Ohno, K.; Morinaga, T.; Koh, K.; Tsujii, Y.; Fukuda, T. *Macromolecules* **2005**, *38*, 2137–2142.
- (18) Barbey, R.; Lavanant, L.; Paripovic, D.; Schuwer, N.; Sugnaux, C.; Tugulu, S.; Kloke, H.-A. *Chem. Rev.* **2009**, *109*, 5437–5527.
- (19) Morinaga, T.; Ohno, K.; Tsujii, Y.; Fukuda, T. *Eur. Polym. J.* **2007**, *43*, 243–248.
- (20) Ohno, K.; Morinaga, T.; Takeno, S.; Tsujii, Y.; Fukuda, T. *Macromolecules* **2006**, *39*, 1245–1249.
- (21) Ohno, K.; Morinaga, T.; Takeno, S.; Tsujii, Y.; Fukuda, T. *Macromolecules* **2007**, *40*, 9143–9150.
- (22) Morinaga, T.; Ohno, K.; Tsujii, Y.; Fukuda, T. *Macromolecules* **2008**, *41*, 3620–3626.
- (23) Ohno, K.; Akashi, T.; Huang, Y.; Tsujii, Y. *Macromolecules* **2010**, *43*, 8805–8812.
- (24) Ladmiral, V.; Morinaga, T.; Ohno, K.; Fukuda, T.; Tsujii, Y. *Eur. Polym. J.* **2009**, *45*, 2788–2796.
- (25) Chiefari, J.; Chong, Y. K.; Ercole, F.; Krstina, J.; Jeffery, J.; Le, T. P. T.; Mayadunne, R. T. A.; Meijs, G. F.; Moad, C. L.; Moad, G.; Rizzardo, E.; Thang, S. H. *Macromolecules* **1998**, *31*, 5559–5562.
- (26) Perrier, S.; Takolpuckdee, P. *J. Polym. Sci., Part A: Polym. Chem.* **2005**, *43*, 5347–5393.
- (27) Barner-Kowollik, C.; Perrier, S. *J. Polym. Sci., Part A: Polym. Chem.* **2008**, *46*, 5715–5723.
- (28) Moad, G.; Rizzardo, E.; Thang, S. H. *Aust. J. Chem.* **2009**, *62*, 1402–1472.
- (29) Boyer, C.; Stenzel, M. H.; Davis, T. P. *J. Polym. Sci., Part A: Polym. Chem.* **2011**, *49*, 551–595.
- (30) Baum, M.; Brittain, W. J. *Macromolecules* **2002**, *35*, 610–615.
- (31) Yoshikawa, C.; Goto, A.; Tsujii, Y.; Fukuda, T.; Yamamoto, K.; Kishida, A. *Macromolecules* **2005**, *38*, 4604–4610.
- (32) Chen, Y. W.; Sun, W.; Deng, Q. L.; Chen, L. *J. Polym. Sci., Part A: Polym. Chem.* **2006**, *44*, 3071–3082.
- (33) Perrier, S.; Takolpuckdee, P.; Mars, C. A. *Macromolecules* **2005**, *38*, 6770–6774.
- (34) (a) Zhao, Y. L.; Perrier, S. *Macromolecules* **2006**, *39*, 8603–8608. (b) Zhao, Y.; Perrier, S. *Macromolecules* **2007**, *40*, 9116–9124. (c) Zhao, Y.; Perrier, S.; Zhou, X.; Huang, Y.; Liu, Q. *Macromolecules* **2009**, *42*, 5509–5517. (d) Huang, Y.; Hou, T.; Cao, X.; Perrier, S.; Zhao, Y. *Polym. Chem.* **2010**, *1*, 1615–1623.
- (35) Peng, Q.; Lai, D. M. Y.; Kang, E. T.; Neoh, K. G. *Macromolecules* **2006**, *39*, 5577–5582.
- (36) Stenzel, M. H.; Zhang, L.; Huck, W. T. S. *Macromol. Rapid Commun.* **2006**, *27*, 1121–1126.
- (37) Wang, G.-J.; Huang, S.-Z.; Wang, Y.; Liu, L.; Qiu, J.; Li, Y. *Polymer* **2007**, *48*, 728–733.
- (38) Li, C. Z.; Benicewicz, B. C. *Macromolecules* **2005**, *38*, 5929–5936.
- (39) Li, C.; Han, J.; Ryu, C. Y.; Benicewicz, B. C. *Macromolecules* **2006**, *39*, 3175–3183.
- (40) Rowe-Konopacki, M. D.; Boyes, S. G. *Macromolecules* **2007**, *40*, 879–888.
- (41) Tsujii, Y.; Ejaz, M.; Sato, K.; Goto, A.; Fukuda, T. *Macromolecules* **2001**, *34*, 8872–8878.
- (42) Li, D. L.; Luo, Y. W.; Li, B.-G.; Zhu, S. P. *J. Polym. Sci., Part A: Polym. Chem.* **2008**, *46*, 970–978.
- (43) Roy, D.; Guthrie, J. T.; Perrier, S. *Macromolecules* **2005**, *38*, 10363–10372.
- (44) Raula, J.; Shan, J.; Nuopponen, M.; Niskanen, A.; Jiang, H.; Kauppinen, E. I.; Tenhu, H. *Langmuir* **2003**, *19*, 3499–3504.
- (45) Hong, C.-Y.; You, Y.-Z.; Pan, C.-Y. *Chem. Mater.* **2005**, *17*, 2247–2254.
- (46) (a) Xu, G. Y.; Wu, W.-T.; Wang, Y. S.; Pang, W. M.; Zhu, Q. R.; Wang, P. H.; You, Y. Z. *Polymer* **2006**, *47*, 5909–5918. (b) Rotzoll, R.; Vana, P. *J. Polym. Sci., Part A: Polym. Chem.* **2008**, *46*, 7656–7666.
- (47) Park, J.; An, K.; Hwang, Y.; Park, J.-G.; Noh, H.-J.; Kim, J.-Y.; Park, J.-H.; Hwang, N.-M.; Hyeon, T. *Nature Mater.* **2004**, *3*, 891–895.
- (48) Yoshinaga, K.; Hidaka, Y. *Polym. J.* **1994**, *26*, 1070–1079.
- (49) Im, J.-S.; Lee, J.-H.; An, S.-K.; Song, K.-W.; Jo, N.-J.; Lee, J.-O.; Yoshinaga, K. *J. Appl. Polym. Sci.* **2006**, *100*, 2053–2061.
- (50) Bartholomew, C. H.; Agrawal, P. K.; Katzer, J. R. *Adv. Catal.* **1982**, *31*, 135–242.
- (51) Calderone, V. R.; Schütz-Widoniak, J.; Bezemer, G. L.; Bakker, G.; Steurs, C.; Philipse, A. P. *Catal. Lett.* **2010**, *137*, 132–140.
- (52) (a) Perrier, S.; Takolpuckdee, P.; Westwood, J.; Lewis, D. W. *Macromolecules* **2004**, *37*, 2709–2717. (b) Takolpuckdee, P.; Mars, C. A.; Perrier, S.; Archibald, S. J. *Macromolecules* **2005**, *38*, 1057–1060.
- (53) Hui, A. W.; Hamielec, A. E. *J. Appl. Polym. Sci.* **1972**, *16*, 749–769.
- (54) Fukuda, T.; Terauchi, T.; Goto, A.; Ohno, K.; Tsujii, Y.; Miyamoto, T.; Kobatake, S.; Yamada, B. *Macromolecules* **1996**, *29*, 6393–6398.
- (55) Ohno, K.; Koh, K.; Tsujii, Y.; Fukuda, T. *Angew. Chem., Int. Ed.* **2003**, *42*, 2751–2754.
- (56) Barner-Kowollik, C.; Buback, M.; Charleux, B.; Coote, M. L.; Drache, M.; Fukuda, T.; Goto, A.; Klumperman, B.; Lowe, A. B.; Mcleary, J. B.; Moad, G.; Monteiro, M. J.; Sanderson, R. D.; Tonge, M. P.; Vana, P. *J. Polym. Sci., Part A: Polym. Chem.* **2006**, *44*, 5809–5831.
- (57) Gubin, S. P., Ed. *Magnetic Nanoparticles*; Wiley-VCH Verlag GmbH & Co. KGaA: Weinheim, 2009; p 466.